

Higher Wood Density Lowers Feedstock Cost and Has Minimal Impact on Biomass Conversion to Biofuels

Raphael AP Ployet, Chanaka Roshan. Abeyratne, Robin J. Clark, Hari B. Chhetri, Doug Hyatt, Miguel Rodriguez, Jr., Sara Jawdy, Dan Xie, Kallysa Taylor, Morgan Davies, Venkataramana R. Pidatala, Anne E. Harman-Ware, Renee M. Happs, Alberto Rodriguez, Trey K. Sato, Erin G. Webb, Stephen P. DiFazio, Jin-Gui Chen, Gerald A. Tuskan, Wellington Muchero, and Brian H. Davison*



Cite This: *ACS Sustainable Chem. Eng.* 2026, 14, 6277–6290



Read Online

ACCESS |



Metrics & More



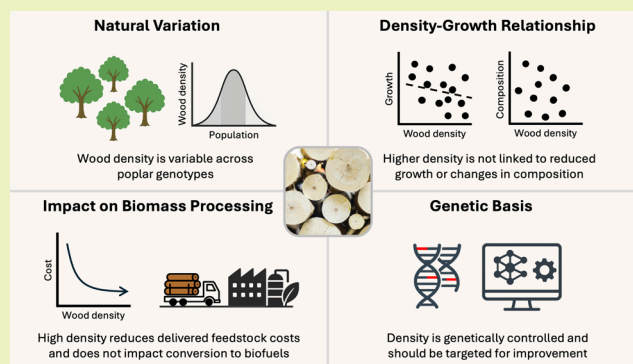
Article Recommendations



Supporting Information

ABSTRACT: Poplar and other woody feedstocks have the potential to provide up to 200 million tons of biomass per year that can be converted to liquid fuels. Most forestry strategies that aim to increase biomass productivity per hectare rely on short rotation plantations of fast-growing varieties. The improvement of the wood density as a key trait itself has largely been overlooked. We evaluated natural variation in wood density across a population of genetically diverse *Populus trichocarpa* trees grown in a common garden. Wood density varies greatly within this population but is heritable; higher wood density was not systematically associated with reduced growth, challenging assumptions of a trade-off between wood density and biomass accumulation. Furthermore, denser wood led to significant improvements throughout the supply chain including lowering biomass production and transportation costs. Higher density did not correlate with changes in biomass composition. Density did not impact bioconversion in the two feedstock-to-fuel pipelines tested (pretreatment by ionic liquids and fermentation to bisabolene or soaking in aqueous ammonia and fermentation to ethanol) on a representative subset of poplars. These findings highlight wood density as a promising breeding target for accelerating the development of high-yielding, conversion-efficient bioenergy crops and as an avenue for increasing land-use efficiency and reducing biomass transportation cost.

KEYWORDS: wood density, biofuels, biomass pretreatment, ammonia pretreatment, ionic liquids, biomass productivity, feedstock costs, poplar



1. INTRODUCTION

The realization of the circular bioeconomy at a large scale will require the addition of significant quantities of reliable low-cost cellulosic feedstocks. Collectively, these feedstocks have the potential of providing 0.7–1.7 B ton/y at a cost up to \$70/ton delivered.¹ Poplar and other woody feedstocks could provide up to 200 million tons per year in the United States alone.¹ Understandably, a lower cost of the delivered feedstock will directly allow for a lower final biofuel or bioproduct cost. One advantage of woody crops is that they have a higher bulk volumetric density than herbaceous or agricultural residues; this should allow a lower transportation cost, as more biomass can be loaded per truck.

The selection of highly productive clones and optimization of planting density have been the main strategies to increase biomass yield per area to reduce biomass production costs.^{2–4} In addition to feedstock costs, pretreatment and conversion significantly contribute to fuel costs. For bioenergy applications

such as thermochemical conversion (i.e., combustion, pyrolysis, and gasification), increasing energy density of the feedstocks using methods such as pelletization has proven to be efficient to reduce transportation/storage costs and ensure uniformity in the biomass supplied.^{5,6} While it is a critical step in the feedstock supply chain, the cost of thermal and mechanical treatments also needs to be considered in the full life cycle emissions of the resulting bioproducts.

In the forestry sector, wood density is considered one of the most important traits because it is variable, relates to yield and quality, and has high heritability (i.e., it is amenable to genetic

Received: October 27, 2025

Revised: February 26, 2026

Accepted: February 26, 2026

Published: March 24, 2026



improvement). Wood density is a measurement of the ratio of wood dry mass to green volume.⁷ Wood density depends on parameters such as age (i.e., juvenile vs mature wood), duration of secondary growth (i.e., sapwood vs heartwood), and stress (e.g., tension wood). Density varies across species, within species, and along climate gradients. In perennial biomass crops, wood density has been shown to vary from 0.25 to 0.5 g/cm³ in hybrid poplars^{8,9} and from 0.35 to 0.6 g/cm³ in eucalyptus,^{10–13} while some of the densest woods such as ebony and “ironwoods” commonly exceed 0.8 g/cm³.^{14–16} Wood density is important for applications such as pulp and lumber, relating to traits such as pulp yields,¹⁷ and increasing density can reduce the cost per ton of pulp.^{18,19}

Several reports have suggested an absence or only a weak negative correlation between wood density and growth parameters in poplar,²⁰ willow,²¹ and eucalyptus,^{22,23} suggesting that it is possible to improve wood density without compromising yield. The genetic component usually explains a significant proportion of the variation in wood density across populations of eucalyptus,²³ poplar,⁹ spruce,²⁴ fir,²⁵ and pine.²⁶ Cornelius²⁷ compiled individual-tree narrow-sense heritability and additive genetic coefficient of variation of seven traits of forest trees and found that wood density tended to have the highest heritability of all traits considered, with a median of 0.48 calculated across 67 studies. In a half-sib family of eucalyptus, Grattapaglia et al.²³ found that density had a higher heritability (estimated between 0.5 and 0.7) than stem diameter (individual-tree heritability of 0.31) and quantitative trait loci (QTLs) were mapped for that trait explaining close to 25% of the phenotypic variation.

The lignocellulosic biomass obtained from wood and agricultural residues is made of cell walls, a composite material composed of multiple polymers—mainly cellulose and hemicellulose comprised of sugars and lignin from phenolics.²⁸ The conversion to biomass-derived chemicals and other bioproducts requires overcoming the recalcitrance of the lignocellulose, which is achieved using a multiple-step pretreatment process. First, by deconstructing, the cell walls are deconstructed into metabolizable compounds such as sugars in hydrolysates followed by their bioconversion into ethanol or other bioproducts. The first step to produce hydrolysates is generally a combination of mechanical, chemical, and enzymatic pretreatment of the biomass. Among the technologies created to loosen the cell wall polymers and increase accessibility for biomass degrading enzymes, two thermochemical pretreatments employing either soaking in aqueous ammonia (SAA) or ionic liquids have been proposed for biofuel production.^{29–33} SAA pretreatment uses ammonia as a catalyst, which induces partial depolymerization of the hemicellulose and lignin and saponification of ester bonds, leading to changes in the structure of the cell walls improving enzyme access to the polysaccharides.²⁹ On the other hand, pretreatment with ionic liquids containing cholinium cations and amino acid anions as catalysts, e.g., cholinium lysinate ([Ch][Lys]), delignifies cell walls and reduces cellulose crystallinity,³⁴ producing swollen cell walls that are more amenable to enzymatic hydrolysis. Hydrolysates from pretreated biomass can be converted to fuel using genetically engineered bacteria and yeasts, such as *Zymomonas mobilis* and *Saccharomyces cerevisiae* for ethanol production³⁵ or the red yeast *Rhodospiridium toruloides* for bisabolene production.³⁶ It is known that the efficacy of conversion is heavily dependent on the feedstock type and composition, the

pretreatment process, and the microbial conversion host; however, the effect of density on the conversion of woody biomass to biofuels has not yet been assessed.

In this study, we examine whether manipulating the wood density would be an avenue for reducing the cost of biofuel production from poplar biomass. We use population-wide data collected from a panel of 1089 black cottonwood poplar (*Populus trichocarpa*) natural variants planted in a common garden, to analyze the variation in wood density and, through a techno-economic analysis, estimate the effect of increasing wood density on the cost of biomass production and transport. To determine whether wood density can be increased without penalty on biomass productivity, we evaluate the phenotypic and genetic correlations between density and biomass productivity and biomass composition-related traits. Biomass samples from a subset of genotypes chosen for contrasting wood densities were then converted to biofuels through two different approaches. One approach used deconstruction with SAA followed by fermentation of the hydrolysates to ethanol using xylose-fermenting *S. cerevisiae* or *Z. mobilis*. The second approach used a cholinium lysinate ionic liquid followed by conversion to bisabolene using an engineered red yeast. We provide evidence that wood density is a critical trait for biorefinery economics and that it should be considered in future breeding programs to reduce costs by boosting biomass productivity and feedstock densification.

2. MATERIAL AND METHODS

2.1. Plant Material, Growth Data, and Sample Collection

Growth data and wood biomass samples were collected from a population of 1089 black cottonwood genotypes (*P. trichocarpa*) assembled from native stands to encompass the central portion of the natural range of the species, stretching from 38.8° to 54.3° N latitude from California, USA, to British Columbia, Canada. Trees were planted in a common garden located in Clatskanie, Oregon, USA (46°6′11″N 123°12′13″W). Establishment of the common garden, growth conditions, and site maintenance have been described by ref 37. Tree height was recorded when trees were 3 years old, and stem diameter at breast height (DBH) was measured when trees were 4 years old. To estimate wood density and composition, two sets of samples were collected when trees were 4 years old: 4.3 mm increment core samples collected from 584 genotypes and stem disks collected from 594 genotypes through destructive sampling. Total fresh weight and fresh volume were measured by water displacement for the whole stem (with and without bark). Then, cores and stem disks were dried in an oven at 94 °C until the weight came to a steady state. Wood density was calculated as the dry weight divided by the green volume (wood specific gravity) using a gravimetric approach or, for estimating the average stem density of fresh material, considering the fresh weight of the whole stem divided by the fresh volume of the whole stem.

In order to collect a larger amount of material required for bioconversion pipelines, a subset of trees from the population was destructively sampled at 10 years old; sections of the trunk were collected, oven-dried, debarked, and chipped using a woodchipper, and then, an aliquot (large chips) was milled to a fine powder using a Thomas Wiley 4 Mill with floor stand (Model 1188Y51, Thomas Scientific, Swedesboro, NJ). Each sample was milled in two consecutive cycles: 10-mesh size and 20-mesh size.

2.2. Wood Composition Analysis

For compositional analysis, we used dried milled core samples. Milled samples (as above) were destarched and extracted with ethanol as previously described.³⁸ Lignin content and S/G ratio were determined by the pyrolysis molecular-beam mass spectrometry (py-MBMS) analysis, and sugar contents (glucose and xylose release) were

characterized using a saccharification assay. These assays were conducted at the National Laboratory of the Rockies (Golden, CO) and were previously described in ref 39. Cell wall sugar hydrolysates and total cell wall sugar content characterization using NMR were conducted on core samples collected from 10 year old trees, following procedures previously described.⁴⁰

2.3. Techno-Economic Analysis

We simulated the production and transport using trunk diameters at breast height at age 7 (DBH7) and wood densities within the measured range of the population. The three DBH7 values in this simulation study included 15, 20, and 25 cm with wood density values ranging from 0.2 to 0.7 g/cm³. The trees in this study would be harvested at age 7, with an estimated height of 18.3 m (60 ft), allowing for two 20 ft cuts to be obtained from each stem. The supply chain configuration modeled in this study—transportation of logs followed by size reduction operations within the biorefinery complex—was chosen to minimize costs while preserving biomass quality, since chips degrade more rapidly than logs. Transportation of the logs to the refinery was simulated using semitrucks equipped with log trailers designed to carry two stacks of 20-foot logs. The trailer's payload is constrained by the quantity of logs that can fit in a stack, as well as the weight of the logs. The maximum number of logs that could fit on a trailer by volume was determined by calculating the cross-sectional area of the log and evaluating it against the area of the payload's width and height, which is approximately two stacks measuring 2.4 m × 2.4 m (8 ft × 8 ft), while assuming a stacking efficiency factor of 75–80%. The wet weight of the logs was calculated using the log volume, wood density, and assumed moisture content of 45%. The geometric model of a conical frustum, as illustrated in eq 1, was used to estimate the log volume, where h represents the length of the log, R is the diameter of the large end of the log, and r is the diameter of the small end of the log to estimate the log volume.

$$\text{volume} = 1/3\pi h(R^2 + Rr + r^2) \quad (1)$$

To calculate the harvestable feedstock yield per hectare, we estimated the yield based on a planting density of 19,977 trees per hectare (equivalent to 800 trees per acre), with each stem yielding two 20 foot logs. Log volume was calculated using eq 1, considering a diameter at breast height (DBH) ranging from 15 to 25 cm. Log weight was then determined using the calculated log volume and wood density, which varied from 0.2 to 0.7 g/cm³. It is evident that both wood density and tree size or growth significantly influence yield, as summarized in Table S1. Using the wet weight of the logs and the calculated maximum number of logs based on the cross-sectional area, we calculated the payload weight. The maximum payload was set at 31.2 mg of wet weight, which corresponds to a maximum of 17.2 mg when accounting for moisture content. The resulting payload weights for different densities and DBH7 values are presented in Table S2. The supply shed configuration was based on the methodologies outlined by Clark and Webb.⁴¹ The daily demand for feedstock was set at 2000 dry tons, with operational uptime established at 90% and a 10% dry matter loss assumed within the system. In addition, two supplementary studies using 1500 and 2500 dry tons per day were conducted to test the impact of the refinery size. A harvest rotation period of 7 years was employed. It was projected that approximately 8% of the landscape surrounding the refinery would be dedicated to feedstock cultivation, with fields randomly dispersed throughout the supply shed.

Economic parameters related to establishment and maintenance, including land preparation, planting, fertilizers, and chemicals, were sourced from the USDOE Billion Ton Report¹ and are summarized in Table S3. The cost is presented in units per hectare. Harvesting and transportation processes were modeled using the Integrated Biomass Supply Analysis and Logistics (IBSAL 2.0) framework in Python. The harvesting setup includes crews consisting of two feller bunchers, five skidders, and three delimeter/loaders, resulting in an operational cost of \$1828 per hour. This crew could harvest 58 dry Mg per hour over an operational year of approximately 200 working days. Transport logistics were modeled using semitrucks with log trailers, with payload

capacity constrained by both weight and volume limitations. Each transportation crew comprises one loader and five trucks, also operating on the same annual schedule of approximately 200 working days. Loading and unloading time was set to be random with a mean of 25 min, with an operational cost of \$626 per hour for a crew of one loader at the field site and five trucks.

2.4. Biomass Deconstruction with Soaking in Aqueous Ammonia Pretreatment and Fermentation of Hydrolysates with *Z. mobilis* and Engineered Yeast

The analysis of the selected subset of six genotypes with high and low densities is described below in Section 3.4. Milled poplar samples were pretreated and solubilized using a modified soaking in aqueous ammonia (SAA) and enzymatic hydrolysis as described elsewhere.³³ In brief, milled biomass was treated with 18% diluted ammonium hydroxide at 75 °C. Dried SAA-pretreated poplar samples were loaded into tubes at 7% glucan loading in potassium phosphate buffer. Hydrolysis was performed using cellulase (Novozymes NS 22257) and xylanase (Novozymes NS 22244) enzymes.

Hydrolysate fermentations were carried out largely as previously described using the Challenge Technology (Springdale, AR, USA) AER-800 respirometer system.^{33,42} The yeast strain GLBRCY1455, which was engineered to ferment xylose,^{33,43} and xylose-fermenting *Z. mobilis* 2032⁴⁴ from the American Type Culture Collection (PTA-6977) were used. At the end of the experiment, cultures were harvested to measure the final cell density and centrifuged to collect the supernatant for metabolomic analysis. Supernatant glucose, xylose, and ethanol concentrations were determined by high-performance liquid chromatography (HPLC) and refractive-index detection (RID) as previously described.⁴⁵

2.5. Biomass Deconstruction with Ionic Liquids and Conversion of Ionic Liquid-Pretreated Hydrolysates with *R. toruloides*

The ionic liquid cholinium phosphate was used as pretreatment solvent at a 5 wt % concentration in water and a bisabolene-producing strain of *R. toruloides* (GB2⁴⁶) was cultivated in the resulting hydrolysates following previously described protocols that include biomass preparation, pretreatment, enzymatic hydrolysis, fermentation and data analysis, as part of a miniaturized feedstocks-to-fuels pipeline.^{47,48}

2.6. Estimation of Genetic Control and Pairwise Genetic Correlation for Density, Biomass, and Wood Composition Traits

We calculated QTL effects using a whole-genome regression approach in which genome-wide single nucleotide polymorphism (SNP) markers are used as proxies for QTLs to predict the resulting trait value.⁴⁹ We obtained genotype data for 431,668 biallelic SNPs segregating in a collection of 1492 *P. trichocarpa* accessions. Details on sequence alignment and variant calling on the population are provided in a previous study.⁵⁰ Briefly, the sequences were aligned to the v4 reference genome using BWA-MEM, and the variants were called with GATK HaplotypeCaller. Individuals that were highly clonal or had >10% missing SNPs were removed. Additionally, SNP positions with more than 15% missing data were excluded. The resulting set was further filtered by removing SNPs with minor allele frequency (MAF) below 0.05 or showing a severe departure from Hardy–Weinberg equilibrium. Only a subset of accessions had both genotypic and phenotypic data available for genomic prediction, with the number of accessions ranging from 479 to 915 depending on the phenotype (Table S4). Missing SNP dosages were imputed using the method implemented in the “Amat” function of the sommer R package,⁵¹ and the final genotype data set along with the respective trait values were supplied as inputs to a Bayesian ridge regression model for genomic prediction as per de los Campos et al.⁵² The statistical model was specified as in eq 2:

$$y = \mu + W\beta + e \quad (2)$$

where y is the vector of phenotypic values, μ is the overall mean, W is the marker genotype matrix (centered and standardized) with each cell representing minor allele dosage for individuals (rows) for SNP markers (columns), β is a vector of marker effects with a common Gaussian prior, and $e \sim N(0, \sigma_e^2 I)$ is the residual error with I representing the identity matrix. The Gibbs sampler was run for 1000 iterations with a burn-in of 100 iterations and a thinning interval of 10 to reduce autocorrelation. Predictive ability was quantified as the Pearson correlation coefficient (PCC) between predicted and observed trait values in the test set using fivefold cross-validation. To evaluate whether the predictive ability obtained was significantly greater than expected by chance, for each trait, we randomly permuted phenotype labels 99 times and repeated the above estimation method of PCC to obtain a null distribution. This was used to obtain an empirical p -value for the observed predictive ability. The pairwise genetic correlation was estimated as PCC between predicted trait values for each trait pair, and the empirical p -value for the genetic correlation statistic was obtained using a null distribution derived from permuted iterations. Narrow-sense heritability (h^2) for all traits was calculated based on additive genetic (σ_a^2) and residual (σ_e^2) variance estimates obtained by fitting the following GBLUP model (eqs 3 and 4).

$$y = 1\mu + Za + e \dots (\text{GBLUP}) \quad (3)$$

$$h^2 = \frac{\sigma_a^2}{(\sigma_a^2 + \sigma_e^2)} \quad (4)$$

Here, y , μ , and e vectors are the equivalent to the genomic prediction model and the vector a represents genome estimated breeding values (GEBVs) for genets modeled by the Z incidence matrix. The additive genetic effect is modeled as $a \sim N(0, \sigma_a^2 G)$. The pairwise additive genetic relatedness among genets was modeled with a genomic relationship matrix G , which was estimated using the same set of SNPs used in the genomic prediction model as per (VanRaden, 2008). Estimation of pairwise relationship matrices, solving linear mixed model equations, obtaining REML estimates of variance components, and obtaining standard errors of estimates were estimated per methods implemented in the R-package sommer v4.1.5.⁵¹

3. RESULTS AND DISCUSSION

3.1. Wood Density Is a Variable Trait in *P. trichocarpa*

To study the variation of wood density, we collected increment core samples and stem disk samples from 584 field-grown *P. trichocarpa* natural variants. Figure 1 shows the density distributions across the population. Core samples had a minimum wood density of 0.312 g/cm³ and maximum density of 0.505 g/cm³, with a median at 0.398 g/cm³ (Figure S1). A similar distribution was obtained on disk samples, with minimum and maximum values of 0.312 and 0.518 g/cm³, respectively, and a median of 0.400 g/cm³. These values are within the range previously observed in poplar, typically varying from 0.300 to 0.500 g/cm³,^{20,53} with a mean density of 0.406 g/cm³ previously measured on a population of 330 *P. trichocarpa* and reported by Porth et al.⁵⁴

As expected, wood density measurements from core and disk samples agreed, with a high correlation $r = 0.94$ ($p < 0.001$; Figure S2) showing that despite within-tree variations for a small proportion of the genotypes, we were able to accurately capture the population-wide density values using increment core samples. Previous studies have shown that density varies within the stem, from pith to bark, and this likely contributed to the minor variations observed between our core and disk samples. The whole-stem density (considering fresh weight of the stem tissues) was overall much lower ranging from 0.062

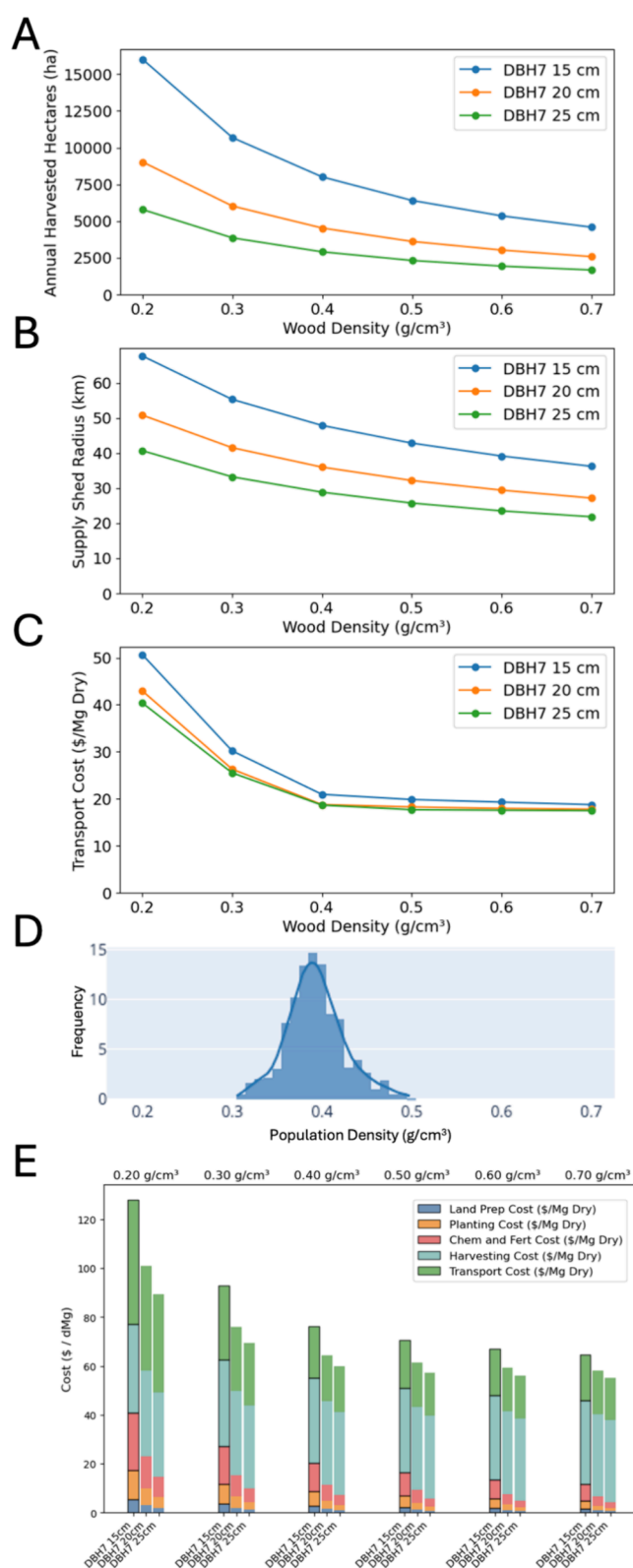


Figure 1. Techno-economic analysis of the effect of density on biofuel production cost. (A) Annual harvest requirement in hectares for different density values observed in the population of *P. trichocarpa* planted in the common garden Clatskanie (OR) and three classes of log diameters (DBH of 15, 20, or 25 cm) is considered harvest at year 7. (B) Supply shed radius is in kilometers for different density values and each log diameter. (C) Estimated biomass transportation cost within the radius of the supply shed in relation to wood density for logs of different diameters. (D) Distribution of the density values

Figure 1. continued

observed in the population. (E) Total feedstock cost was estimated for these different density values and log diameter with a breakdown of the contributing costs.

g/cm^3 to $0.820 \text{ g}/\text{cm}^3$, with a median of $0.145 \text{ g}/\text{cm}^3$ (Figure S2). The whole-stem density did not correlate with wood density measured on core and disk samples collected at breast height. This result is not surprising, as, in addition to the moisture content that can interfere with the measurement, averaging the density across all sections of the stem leads to a larger error when estimating wood density. Multiple studies showed that the density is highly variable along the height gradient of the main stem. Beaudoin et al.⁵³ showed that wood density in *Populus deltoides* \times *Pinus nigra* hybrids is usually higher at the base of the stem, then drops going upward reaching minimum at midheight, and increases again toward the top, likely due to major differences in vessel density. Typically, cell wall thickness, xylem conduit size, and fiber properties are the main morphological parameters that determine wood density.⁵⁵ Seasonal variations in growth

patterns and maturity of the tree can lead to changes in these xylem morphological properties, with some drastic variations in the case of latewood vs early wood, for example, all of these inputs impact the overall wood density.^{56,57} In this study, it cannot be ruled out that differences in maturity could be a factor in the observed variation in density; however, the observed low correlation between DBH (stem diameter) and density (Figure 2) suggests that a difference in the proportion of juvenile to mature wood is not a determining factor. Across the 584 genotypes considered, wood density had a relative standard deviation (RSD) of 8.2% when measured on core samples. The RSD was lower than for height (RSD = 25.7%, $n = 569$ genotypes) and DBH (RSD = 33.2%, $n = 507$ genotypes) but higher than for lignin content (RSD = 5.8%, $n = 469$ genotypes) measured on that same set of genotypes. The range in phenotypic values is comparable to 9.8% variation found across different hybrid crosses of poplars by Pliura et al.,²⁰ highlighting the large intraspecific variation in *P. trichocarpa*.

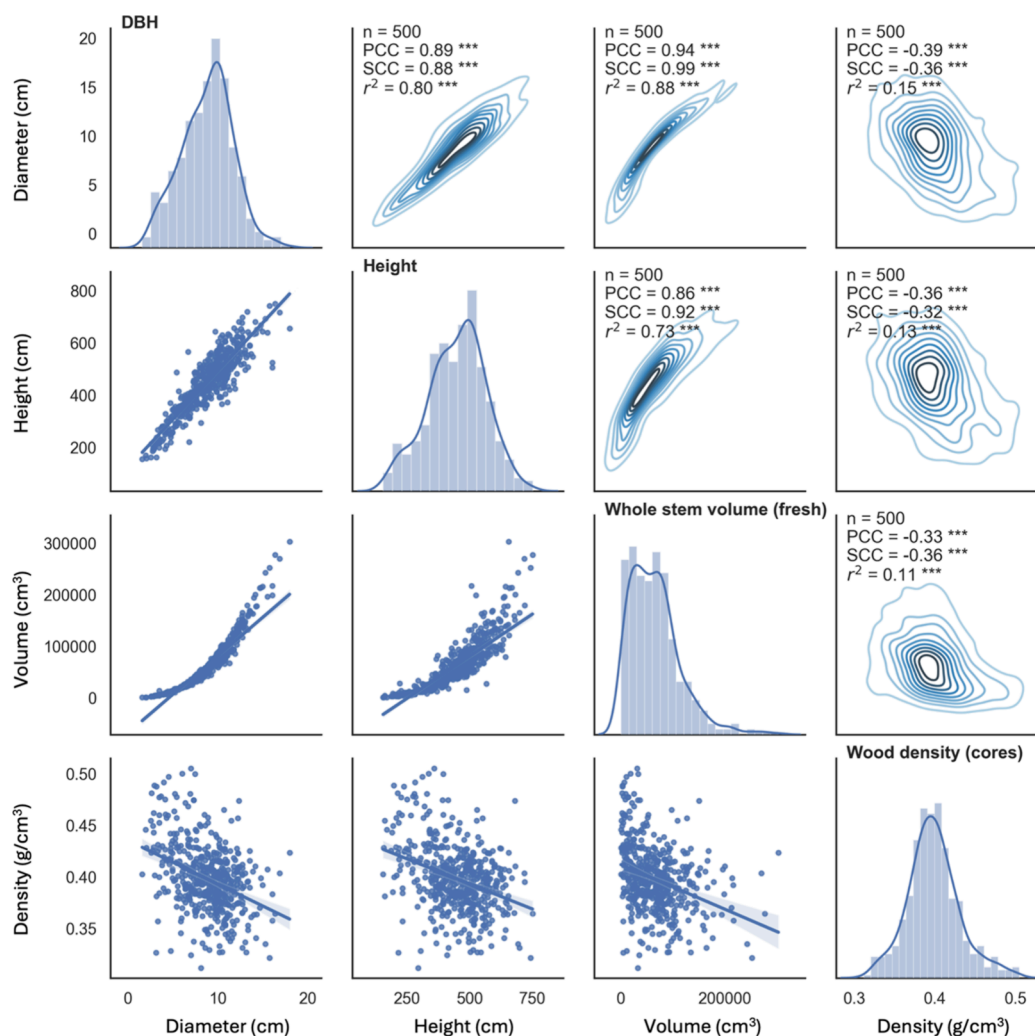


Figure 2. Relationship between wood density measured on core samples and biomass yield-related traits. Scatter plots are shown below the diagonal, relative sample frequency trait distributions are shown on the diagonal, and correlation metrics are shown above the diagonal. DBH, diameter at breast height; n , number of genotypes considered; PCC, Pearson correlation coefficient; SCC, Spearman correlation coefficient; r^2 , coefficient of determination; * $p < 0.05$, ** $p < 0.01$, *** $p < 0.001$.

3.2. Increase in Wood Density Has the Potential to Reduce Costs for Biomass Production and Transportation

Planting genotypes with higher density has the potential to reduce the cost of biomass production, via not only an increase in biomass yield per unit area but also a decrease in field establishment, maintenance, harvesting, and transportation costs. We performed a techno-economic analysis modeling the production and transport of biomass from the field, for density values ranging from 0.2 to 0.7 g/cm³. The annual harvest requirement in hectares was significantly influenced by the wood density and the diameter at the breast height (DBH) of the trees (Figure 1a). For example, with a DBH of 20 cm, we observed a substantial reduction in land requirements—from 6017 to 3606 ha—as wood density increased from 0.3 g/cm³ to 0.5 g/cm³. This represents a 40% decrease in the required harvesting area, emphasizing the critical role wood density could play in the sustainability and efficiency of the biomass supply chain. Thus, the annual harvest requirement in ha directly affects the supply shed radius (Figure 1b) required to support the demand of 2000 dt per day. In our analysis, we stipulated that 8% of the land area surrounding the biomass refinery would be dedicated to feedstock production. With higher wood density having a positive effect on the weight of the cargo, larger amounts of biomass can be transported per load, which implies that fewer loads are transported over shorter distances, reducing the overall transportation cost. Altogether, this would lead to a decrease in total biomass cost by an average of 20% (24% for 15 cm logs, 19% for 20 cm logs, and 17% for 25 cm logs; Figure 1e).

Furthermore, both the supply shed radius (Figure 1b) and trailer load capacity (Table S2) are integral components of the transport costs shown in Figure 1c. In this approach, the transport system was modeled using IBSAL,⁴¹ considering trucks with a maximum cargo capacity of 30 tons transporting biomass within the radius of the supply shed. The trailer cargo weight was calculated for logs with a DBH of 15, 20, or 25 cm. The maximum number of logs per load based on volume (maximum capacity of the trailer) was estimated at 448, 264, and 162 logs, for 15, 20, and 25 cm diameter logs, respectively. As expected, the cargo weight increases as a function of density and DBH. For each diameter, an increase in density results in heavier cargo transported to the refinery, leading to a significant decrease in transportation cost up to a wood density of 0.4 g/cm³. Beyond this threshold, transport capacity becomes constrained by weight rather than volume. Within the density range observed in the sampled population, increasing wood density from 0.3 to 0.5 g/cm³ would lead to a decrease of the transport cost of up to 34% for smaller logs and 31% for 25 cm logs (Figure 1c). We also examined the sensitivity to the daily demand value (Figure S3); the qualitative trends are the same with both larger and smaller demand. Moisture content was assumed to be constant as trees would be directly harvested and shipped. Obviously, the moisture content will directly increase the weight of a log in a linear fashion. This would shift the density curves in Figure 1 to the right but will not change our conclusions. Moisture will be influenced by the environment and storage. In alternative supply chain designs where size reduction (i.e., chipping) occurs closer to the production site, transportation costs should be less influenced by wood density; however, the effects of wood density on production costs remain the same.

For all three classes of log diameters considered (15, 20, and 25 cm) and accounting for land preparation, planting, chemical

applications, harvesting, and transportation, a 20% decrease in costs associated with the biomass production could be achieved by increasing wood density from 0.3 to 0.5 g/cm³ (Figure 1e). The cost of harvest could also be decreased to a lesser extent by up to 7% for smaller logs (15 cm) and up to 2.4% for 25 cm diameter logs (Figure 1a). Notably, harvest and transport costs dominate the total expenditure, underscoring the importance of lowering these costs to achieve a more economically viable biomass supply chain. Previous studies have demonstrated that increasing density of the feedstock can have multiple positive effects on the supply chain, largely by reducing the transportation costs, and making handling and storage of biomass easier.⁵⁸ Whether it is biomass originating from dedicated biomass crops or agricultural and forestry residues, increasing the density of biomass by pelletization, for example, makes transportation by road and rail cheaper than for raw untreated biomass.^{59–61} However, because pelletization itself is costly, requiring mechanical and thermal treatment of the biomass, Gunukula et al.⁶² have shown that depending on the supply chain, densifying a low bulk density feedstock like switchgrass does not significantly improve the cost of biofuel production. Alternatively, increasing wood density by leveraging a biological process to increase biomass dry weight per unit area, which will not require additional biomass pretreatment, will have a direct positive impact on the whole supply chain.

3.3. Wood Density Can Be Optimized without a Negative Impact on Wood Biomass Productivity

We then tested the correlation among wood density, DBH, height, and whole-stem volume (fresh volume) across 500 genotypes for which we measured all four traits. As expected, DBH, height, and stem volume were highly positively correlated with $r > 0.8$ and $r^2 > 0.7$ ($p < 0.001$; Figure 2). DBH was proportional to height, while the fresh stem volume had a nonlinear association with DBH and height, as the stem volume is generically defined by the volume of a cone. In contrast, wood density was found significantly but poorly negatively correlated with all other growth parameters ($r > -0.4$, $p < 0.001$) with a low coefficient of determination ($r^2 < 0.2$) compared to other traits. This is consistent with previous studies that have found that wood density is not, or is weakly, correlated to growth parameters in poplar. In poplar hybrids, Pliura et al.²⁰ also found that height, DBH, and stem volume are highly correlated ($r > 0.8$ for DBH vs height; $r > 0.7$ for height vs volume, $p < 0.05$). They also observed a weak negative correlation between density and DBH ($r = -0.44$ to -0.19 , $p > 0.05$), density vs volume ($r = -0.30$ to -0.19 , $p > 0.05$), and density vs height was significant only when height was measured on young (3 years old) trees ($r = -0.59$, $p < 0.05$), while in all other measurements that correlation did not exceed $r = -0.26$. Similarly, Beaudoin et al.⁵³ reported a negative correlation $r = -0.46$ between density and inner bark diameter of the trunk in poplar hybrids. Zhang et al.⁸ did not find a significant correlation between density and these other growth parameters ($r = -0.05$ to -0.16 , $p > 0.05$). These reports confirm our observation that there is a weak trade-off between wood biomass productivity and wood density in poplar and despite that trade-off, it is possible to identify genotypes that combine superior wood density and high growth performance.

Similarly, we estimated the correlation between wood density and wood compositional traits, including lignin-related traits (lignin content and S/G ratio) estimated by py-MBMS

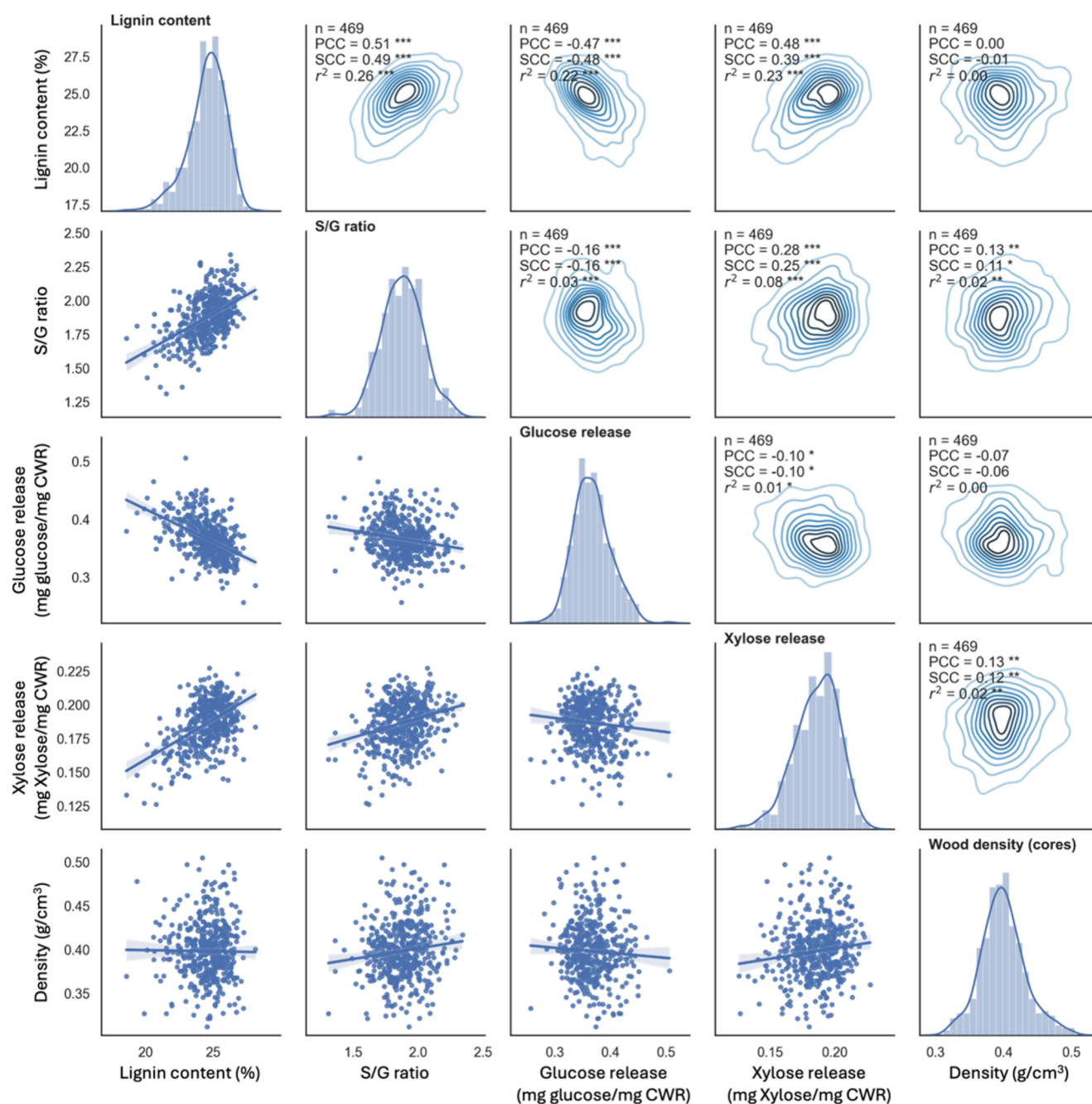


Figure 3. Relation between wood density and biomass composition. These parameters were measured on core samples, scatter plots are shown below the diagonal, relative sample frequency trait distributions are shown on the diagonal, and correlation metrics are shown above the diagonal. CWR, cell wall residue; *n*, number of genotypes considered; PCC, Pearson correlation coefficient; SCC, Spearman correlation coefficient; *r*², coefficient of determination; * *p* < 0.05, ** *p* < 0.01, *** *p* < 0.001.

and the enzymatic release of glucose and xylose from the polysaccharide fraction (cellulose and hemicellulose, respectively) collected from the same genotypes. As expected, a significant positive correlation was observed between lignin content and S/G ratio ($r = 0.51$, $p < 0.001$), as well as a significant negative correlation with enzymatic glucose release ($r = -0.47$, $p < 0.001$), whereas a positive correlation was observed between lignin content and xylose release ($r = 0.48$, $p < 0.001$; Figure 3). Since the enzymatic release of sugars can underestimate the actual sugar content, we quantified the total cell wall sugar content with an acid hydrolysis followed by NMR, on a subset of the population (over 200 genotypes).

Strong correlations were detected among sugars, such as the negative correlation between glucose and xylose ($r = -0.75$, $p < 0.001$; Figure S4), which may reflect a trade-off in carbon allocation between cellulose and xylan. Wood density did not correlate with any of the compositional traits analyzed (all $r^2 < 0.1$), suggesting that selecting genotypes with higher wood density is unlikely to involve changes in wood composition in this population.

To determine whether wood density is under additive genetic control in *P. trichocarpa*, we trained genomic prediction models to estimate the predictive ability for wood density (Figure 4a), growth-related traits (DBH and height; Figure

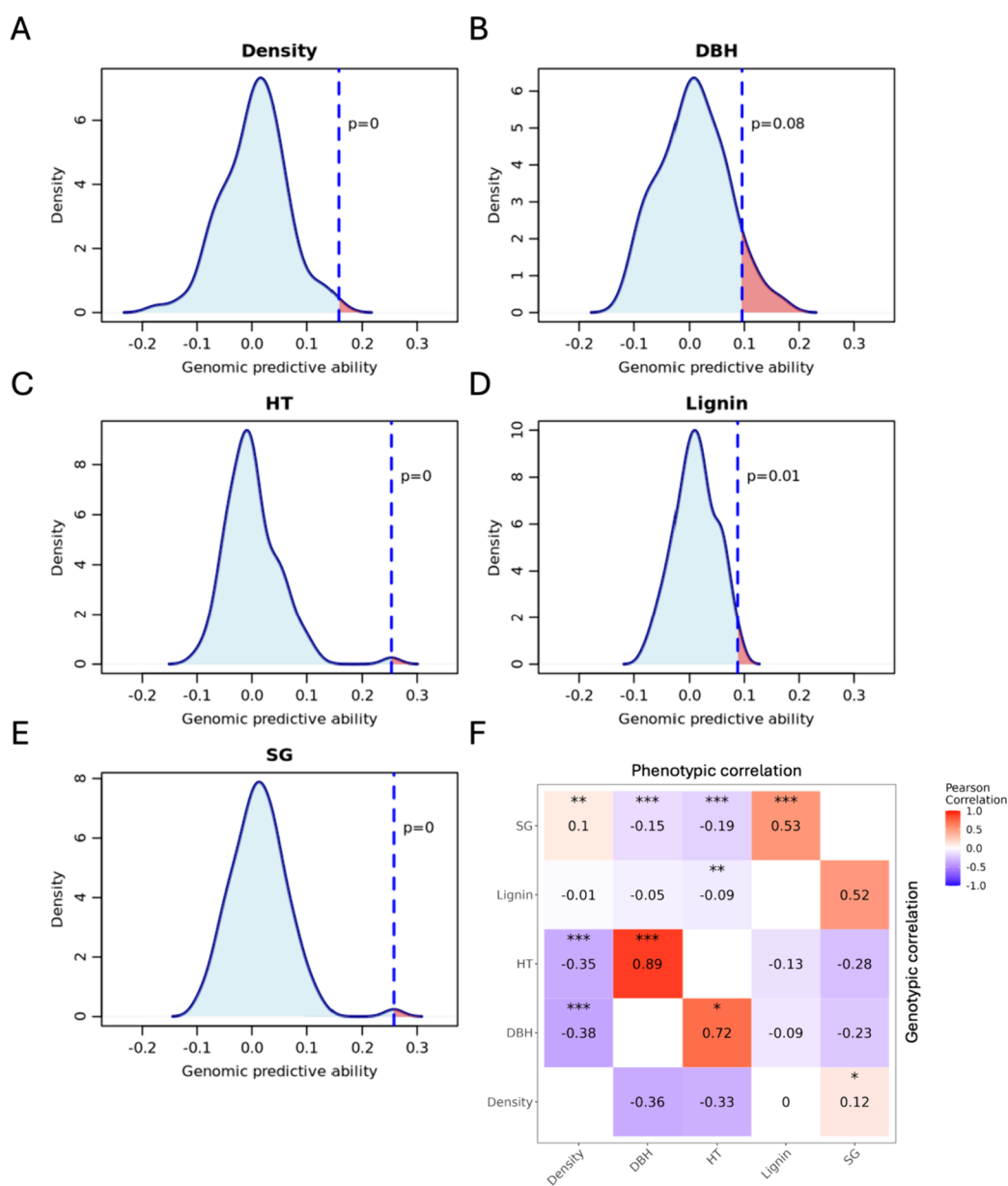


Figure 4. Predictive ability, phenotypic correlations, and genetic correlations for density and traits related to biomass productivity and composition. (A–E) Genomic predictive ability of each trait is indicated with the dashed line indicating the observed genomic predictive ability and the null distribution representing predictive ability estimated using 99 permutations of the trait values (empirical p -values are reported). (F) Heatmap of the genetic correlations (lower triangle) and phenotypic correlations (upper triangle). * $p < 0.05$, ** $p < 0.01$, *** $p < 0.001$.

4b,c), and biomass composition-related traits (lignin content and S/G ratio; Figure 4d,e). Here, 431,668 genome-wide SNP markers were used to capture putative QTL effects and train the prediction model. Estimated SNP effects were then used as proxies for underlying QTL effects to predict the trait value for a given accession. Overall, the predictive ability (i.e., Pearson correlation coefficient between actual vs estimated trait value) for all traits tested was low but significantly greater than zero as demonstrated by estimating empirical p -values based on 99 permutations. This is largely due to the inherent properties of our population (wild accessions with very low relatedness) and the lack of replication. The predictive ability for density was significant (0.16, $p < 0.001$; Figure 4a) and higher than values for DBH (0.095, $p = 0.08$; Figure 4b) and lignin content (0.09, $p < 0.05$; Figure 4b), which are both known to be under substantial additive genetic control.^{63,64} However, the

predictive ability of density was lower than for both height and S/G ratio (both values >0.25 , $p < 0.001$; Figure 4c,e). These findings are consistent with previous studies which discovered that density has a much higher heritability and genetic correlation than DBH and height in poplar.^{8,20} We observed a high estimate of genomic heritability (0.851) for wood density (Table S4). Previous studies have consistently shown that wood density has a high heritability, reaching close to, or exceeding 0.6 in *P. trichocarpa* ($h^2 = 0.558^{34}$), *P. deltoides*,^{65–67} and *Populus euramericana*.⁵³ Our data set lacked replication at the accession level, which likely led to inflated estimates of heritability using a GBLUP model. In addition, for natural accessions used in our study, the G -matrix is largely sparse with a low information content in the off-diagonals for pairwise relatedness. It is known that predictive ability of genomic selection models as used in our study depend both on

Table 1. Average Properties of the Subset of Genotypes Selected for Deconstruction

criteria	density (g/cm ³)	DBH (cm)	height (cm)	fresh stem volume (cm ³)	lignin content (% CWR)	glucose release (mg/mg CWR)	xylose release (mg/mg CWR)
high density ^a	0.434 (0.018)	9.8 (0.6)	497 (28)	72000 (2828)	24.7 (0.38)	0.042 (0.011)	0.0147 (0.0043)
low density ^a	0.346 (0.026)	11.2 (1.6)	504 (23)	97000 (31097)	25.3 (1.51)	0.073 (0.039)	0.0147 (0.0049)
population ^a	0.400 (0.033)	8.7 (2.95)	461 (124)	66720 (54984)	24.5 (1.6)	0.0455 (0.0267)	0.0103 (0.0062)
population min	0.312	1.0	75	1000	17.6	0.0092	0.0007
population max	0.505	18.0	816	655000	28.4	0.1754	0.0549

^aAverage values are presented for each trait above the standard deviation shown in parentheses. The detailed genotype analyses are shown in Table S5.

realized pairwise relatedness and marker-QTL linkage disequilibrium (LD) between individuals in training and test data sets.⁶⁸ In our study, the marker-QTL LD is also expected to be low, as accessions were sampled across the full natural range of *P. trichocarpa*, encompassing diverse genetic backgrounds. This likely explains the mismatch between observed depression in predictive ability and the inflated narrow-sense heritability. This heritability analysis shows that wood density is under significant genetic control, which agrees with previous studies in other species. In addition, the genetic correlations of these traits showed a similar trend to the phenotypic correlations, with the highest genetic correlation found between DBH and height ($r = 0.72$, $p < 0.05$), while density had a relatively low correlation with DBH and height ($r = 0.36$ and $r = 0.33$, respectively, $p > 0.05$; Figure 4f), which agrees with previous studies reporting a weak association between growth parameters and wood density in poplar,^{8,69,70} and other species.^{21–23} Although the genetic correlation between density and S/G ratio was found significant ($r = 0.12$, $p < 0.05$), the absolute value of the correlation was low, and density was not found correlated to lignin content. This also agrees with Porth et al.⁵⁴ who detected a weak phenotypic correlation between density and wood compositional and structural properties in *P. trichocarpa*. In this study, the authors reported significant positive genetic correlations between density and cellulose properties (i.e., % α -cellulose, % holo-cellulose, and % glucose) and a weak but significant negative correlation between density and the total lignin content, suggesting that selecting genotypes with higher wood density would also lead to advantageous properties for cellulosic-derived biofuels (i.e., higher cellulose and lower lignin content⁵⁴).

Our results and the literature suggest that meaningful genetic gains for higher wood density can be obtained in a controlled tree breeding program without significantly interfering with selection goals for growth and wood compositional traits. Although the predictive ability estimated in our study indicates low heritability values for wood density, the population mean for traits with low heritability can still be substantially improved by imposing a more stringent selection intensity (S) as response to selection (R) in the next generation is the product of trait heritability (h^2) and selection intensity ($R = h^2S$). In this context, investigating the duration (number of breeding cycles) that would be required for making the selection gains advised for DBH (15–25 cm) and wood density (0.3–0.5 g/cm³), which would require a replicated proof-of-concept breeding trial for *P. trichocarpa*.

3.4. Wood Density Does Not Impact Biomass Deconstruction and Conversion in Two Alternate Pipelines

The saccharification assay performed at the population level (Figure 3) did not show a significant correlation between changes in wood density and the enzymatic release of sugars (glucose and xylose; Figure 3), which are the primary targets for fermentation to biofuels, suggesting that a higher wood density does not lead to a higher recalcitrance. To investigate the effect of wood density on bioconversion pipelines for biofuel applications, we selected a subset of high and low wood density genotypes for deconstruction (three genotypes for each group) with similar lignin and glucan contents. The high-density group had an average wood density of 0.43 g/cm³, which was significantly higher than the low-density group with an average density of 0.34 g/cm³ (Student's t test, $p < 0.05$; Table 1; Figure S5). These two groups of samples were not significantly different for other phenotypes such as DBH, height, stem volume, lignin content, and enzymatic release of glucose and xylose (Student's t test $p > 0.05$; Table 1; Figure S5; Table S5).

Biomass samples of these three high- or low-density genotypes were deconstructed using two distinct lignocellulosic biomass deconstruction pipelines, either SAA³³ or ionic liquids.³⁴ After SAA and enzymatic hydrolysis, the hydrolysates from the high-density and low-density biomass samples yielded a similar average titer at 80 and 78.9 g/L of glucose, respectively (Figure 5a). When biomass was dissolved using 5% cholinium phosphate as a catalyst, also followed by an enzymatic hydrolysis at 50 °C for 72 h, the glucose yield for high-density biomass samples was in average 30.3 g/L, which was not significantly different from the glucose yield obtained for low-density biomass samples (29.2 g/L, Student's t test $p > 0.05$; Figure 5b). Similarly, xylose concentrations reached 8.3 and 8.1 g/L for high and low-density, respectively (Figure 5b). This agrees with the results obtained for the saccharification assay that included an ethanol extraction to obtain extractive free material, followed by a hot water treatment, and then mild dilute acid treatment during enzymatic hydrolysis. Although one low-density genotype showed higher saccharification efficiency, high- and low-density genotypes had similar glucose and xylose yields (Figure S5). In both the saccharification assay and the ionic liquid pretreatment, we did not detect a trade-off between wood density and xylose release, unlike that reported in willow by Ohlsson et al.²¹ Altogether, our results demonstrate that wood density is not a critical parameter that directly impacts biomass deconstruction into fermentable sugars.

With no significant differences in the glucose titers of the hydrolysates obtained from the pretreatment steps, the

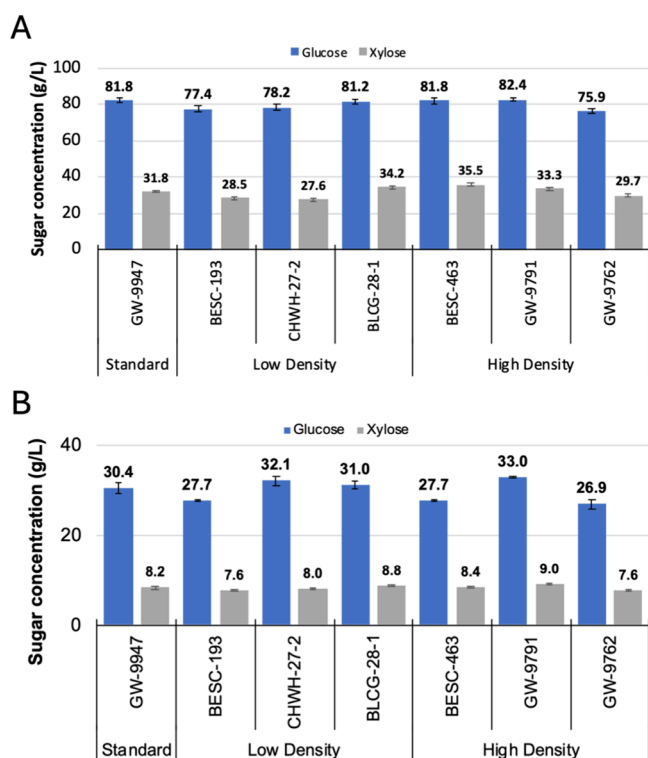


Figure 5. Deconstruction of high- and low-density biomass samples using aqueous ammonia or ionic liquids. (A) Sugar yields were obtained after SAA pretreatment and enzymatic hydrolysis. (B) Glucose yields after pretreatment with cholinium phosphate and enzymatic hydrolysis. Reactions were performed in three to four technical replicates (replication for the pipeline starting from a different subsample), and the standard deviation represents variation across these technical replicates ($n = 4$).

hydrolysates were converted to various biofuels using strains of bacteria or yeast engineered to ferment xylose. Hydrolysates produced from SAA pretreatment were converted to ethanol using *Z. mobilis* strain Zm2032⁴⁴ or *S. cerevisiae* strain GLBRCY1455.⁴³ After the microbial conversion to ethanol, for both *Z. mobilis* and *S. cerevisiae*, as expected, glucose utilization reached close to 100% for all samples with no significant effect of density: 98.6% and 98.4% in average for low- and high-density genotypes, respectively, for Zm2032 (Figure 6a); 99.7% for both low- and high-density genotypes for GLBRCY1455 (Student's t test $p > 0.05$; Figure 6b). Ethanol titers were also not significantly different between low- and high-density derived hydrolysates, with an average of 41.3 and 42.0 g/L for Zm2032, and 50.1 and 51.9 g/L for GLBRCY1455, for low- and high-density genotypes, respectively (Student's t test $p > 0.05$; Figure 6a,b). These fermentation values are consistent with a similar cell density measured across all samples, indicating uniform microbial growth for both strains (Figure 6a,b). As expected, xylose utilization was high for strain GLBRCY1455, also with no effect of sample initial wood density (92.4% utilization for both low- and high-density samples; Figure 6b). For strain Zm2032, it appeared lower (45% in average) and more variable across samples, reaching 47% for low-density genotypes and 43.1% for high-density genotypes (Figure 6a), suggesting a genotype effect due to some other compositional or structural property but not a direct effect of wood density on the conversion of C5 sugars to biofuels.

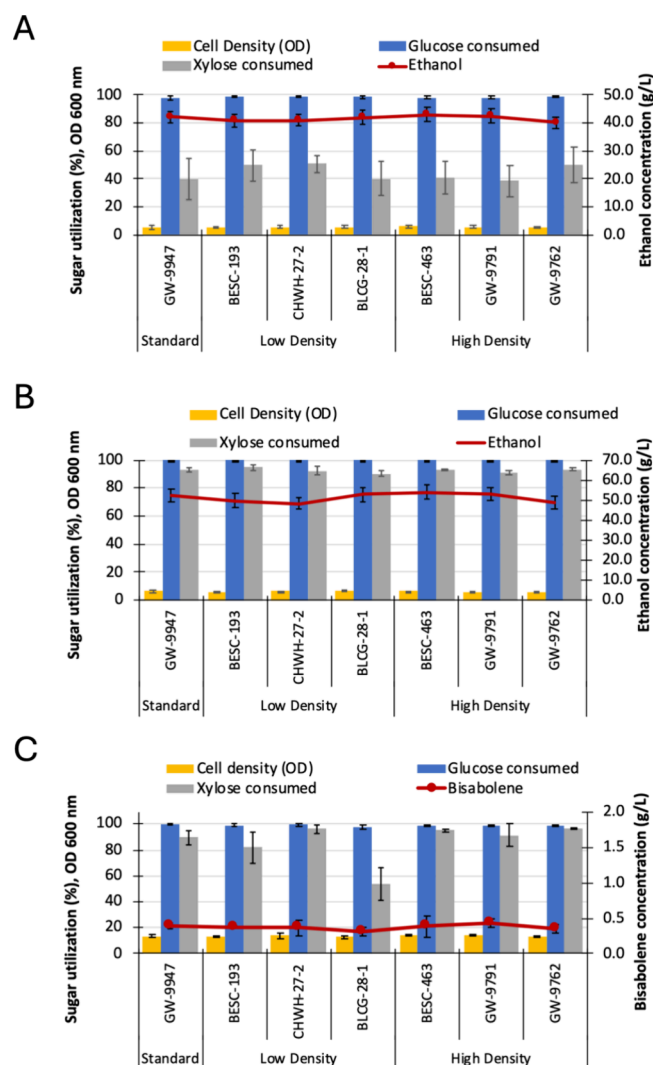


Figure 6. Effect of wood density on the microbial conversion to biofuels. Conversion of hydrolysates obtained from SAA-pretreated biomass using (A) *Z. mobilis* Zm2032, SAA-pretreated biomass using (B) *S. cerevisiae* strain GLBRCY1455, and conversion of hydrolysates obtained from biomass pretreated with cholinium lysinate using (C) *R. toruloides* strain GB2.

Hydrolysates obtained from biomass dissolved using cholinium phosphate pretreatment were converted to bisabolene using an engineered strain of the oleaginous red yeast that is natively capable of utilizing both glucose and xylose (*R. toruloides* named GB2⁴⁶). *R. toruloides* GB2 was able to grow on all samples, as represented by a similar optical density value across all samples (~13–15 OD 600 nm) and displayed similar glucose utilization for high and low-density samples (Figure 6c). Although xylose utilization was more variable, especially for low-density genotypes (average of 94% for high and 77% for low-density, standard deviation low density = 21.5), bisabolene titers were not significantly different between the two groups, ranging from 0.35 to 0.43 g/L for high-density and 0.31 to 0.38 g/L for low-density samples (Student's t test $p > 0.05$; Figure 6c). The bisabolene titers are comparable to those observed in a previous report that showed conversion of poplar hydrolysates obtained using the ionic liquid cholinium lysinate in 1 L Parr reactors by the same strain.⁷¹ Our findings demonstrate that although

genotype-specific variations can impact the microbial conversion of biomass to fuels, under our tested conditions, higher wood density does not lead to an increase in biomass recalcitrance or a detrimental effect on biomass conversion.

Some studies have shown that higher wood density can have a negative impact on biomass deconstruction for pulp for example.⁷² We compared trees of the same species, same age, and with similar wood composition (lignin, cellulose, and xylan content) to ensure no confounding effect caused by significant changes in composition. Our results indicate that higher wood density does not render the biomass more recalcitrant to biofuel conversion. This could be explained by the fact that differences in density are due to changes in cell morphology rather than changes in cell wall composition, which is a major determinant of biomass recalcitrance. These results show that selecting or engineering certain cell morphological traits could permit biomass densification for bioenergy applications, as suggested in monocots by Gallego-Giraldo et al.⁷³

4. CONCLUSIONS

We performed an initial evaluation across the supply chain on the variability and impact of wood density as a key trait for improvement of both yield per unit area and transport costs as well as wood density's effect on processability. Our results show that wood density varies within a single species population of *P. trichocarpa* and the variation was broader than expected with a range from 0.3 to 0.5 g/cm³ with a mean near 0.4 g/cm³. Utilizing the wood density within this range would result in a 32% decrease in transport costs or an absolute decrease of up to \$10/dry Mg, which significantly reduces the biomass delivered cost to \$70/Mg. We note that there is a potential upper limit outside of the observed natural range where the density benefit is restricted due to the current overall weight limits of the trucks. In addition, our analysis indicates that the wood density generally is independent of composition and growth. In the two different feedstock-to-fuel processes studied, density had minor to no effect on the pretreatment and bioconversion. This neutral result is encouraging, as it suggests that the biomass density can be increased with the positive benefits indicated and without a negative impact on the conversion. The results of the genomic prediction models further support the potential to independently breed for density and other desirable traits simultaneously in poplar. This study provides evidence that wood density is an economically valuable and heritable trait that must be prioritized in future breeding programs. Future studies should investigate both the morphological changes and the genetic and metabolic mechanisms underlying the changes in wood density in poplar.

■ ASSOCIATED CONTENT

SI Supporting Information

The Supporting Information is available free of charge at <https://pubs.acs.org/doi/10.1021/acssuschemeng.5c10590> and at the doi below. For phenotype data collected for 584P. *trichocarpa* genotypes grown in a common garden in Clatskanie (Oregon, USA), the datasets are available at <http://doi.org/10.25983/CBI/3012637>.

Tables S1–S5 and Figures S1–S5 (PDF)

■ AUTHOR INFORMATION

Corresponding Author

Brian H. Davison – Center for Bioenergy Innovation and Biosciences Division, Oak Ridge National Laboratory, Oak Ridge, Tennessee 37831, United States; orcid.org/0000-0002-7408-3609; Email: davisonbh@ornl.gov

Authors

Raphael AP Ployet – Center for Bioenergy Innovation and Biosciences Division, Oak Ridge National Laboratory, Oak Ridge, Tennessee 37831, United States; University of Tennessee – Oak Ridge Innovation Institute, University of Tennessee, Knoxville, Tennessee 37996, United States; orcid.org/0000-0003-4809-5988

Chanaka Roshan. Abeyratne – Center for Bioenergy Innovation and Biosciences Division, Oak Ridge National Laboratory, Oak Ridge, Tennessee 37831, United States

Robin J. Clark – Center for Bioenergy Innovation and Environmental Sciences Division, Oak Ridge National Laboratory, Oak Ridge, Tennessee 37831, United States; orcid.org/0000-0002-0217-1124

Hari B. Chhetri – Center for Bioenergy Innovation and Biosciences Division, Oak Ridge National Laboratory, Oak Ridge, Tennessee 37831, United States

Doug Hyatt – Center for Bioenergy Innovation and Biosciences Division, Oak Ridge National Laboratory, Oak Ridge, Tennessee 37831, United States

Miguel Rodriguez, Jr. – Center for Bioenergy Innovation and Biosciences Division, Oak Ridge National Laboratory, Oak Ridge, Tennessee 37831, United States

Sara Jawdy – Center for Bioenergy Innovation and Biosciences Division, Oak Ridge National Laboratory, Oak Ridge, Tennessee 37831, United States

Dan Xie – Great Lakes Bioenergy Research Center, University of Wisconsin-Madison, Madison, Wisconsin 53726, United States

Kallysa Taylor – Great Lakes Bioenergy Research Center, University of Wisconsin-Madison, Madison, Wisconsin 53726, United States

Morgan Davies – Great Lakes Bioenergy Research Center, University of Wisconsin-Madison, Madison, Wisconsin 53726, United States

Venkataramana R. Pidatala – Deconstruction Division, Joint BioEnergy Institute, Emeryville, California 94608, United States; Biological Systems and Engineering Division, Lawrence Berkeley National Laboratory, Berkeley, California 94720, United States

Anne E. Harman-Ware – Center for Bioenergy Innovation, Oak Ridge National Laboratory, Oak Ridge, Tennessee 37831, United States; Biosciences Center, National Laboratory of the Rockies, Golden, Colorado 80401, United States; orcid.org/0000-0002-7927-9424

Renee M. Happs – Center for Bioenergy Innovation, Oak Ridge National Laboratory, Oak Ridge, Tennessee 37831, United States; Materials, Chemical, and Computational Sciences Center, National Laboratory of the Rockies, Golden, Colorado 80401, United States; orcid.org/0000-0001-7139-0083

Alberto Rodriguez – Deconstruction Division, Joint BioEnergy Institute, Emeryville, California 94608, United States; Department of Biomaterials and Biomanufacturing, Sandia

National Laboratories, Livermore, California 94550, United States; orcid.org/0000-0002-4045-0108

Trey K. Sato – Great Lakes Bioenergy Research Center, University of Wisconsin-Madison, Madison, Wisconsin 53726, United States

Erin G. Webb – Center for Bioenergy Innovation and Environmental Sciences Division, Oak Ridge National Laboratory, Oak Ridge, Tennessee 37831, United States; orcid.org/0000-0002-1501-8647

Stephen P. DiFazio – Department of Biology, West Virginia University, Morgantown, West Virginia 26506, United States

Jin-Gui Chen – Center for Bioenergy Innovation and Biosciences Division, Oak Ridge National Laboratory, Oak Ridge, Tennessee 37831, United States

Gerald A. Tuskan – Center for Bioenergy Innovation and Biosciences Division, Oak Ridge National Laboratory, Oak Ridge, Tennessee 37831, United States

Wellington Muchero – Center for Bioenergy Innovation and Biosciences Division, Oak Ridge National Laboratory, Oak Ridge, Tennessee 37831, United States

Complete contact information is available at:

<https://pubs.acs.org/10.1021/acssuschemeng.5c10590>

Author Contributions

R.A.P.P. designed the approach, analyzed the data, and wrote the manuscript; C.R.A. estimated genomic heritability and genetic correlations across traits, trained the genomic prediction models, and contributed significant written portions of the manuscript; H.B.C. participated in phenotypic data collection, and H.B.C. and D.H. carried out genomic variant calling and filtering for all accessions; R.J.C. designed and performed the TEA and contributed to the related section of the manuscript; E.G.W. contributed to the TEA design and reviewed the TEA results; T.K.S. designed the SAA deconstruction and conversion pipeline and contributed to the writing and editing of the manuscript; D.X., K.T., and M.D. performed the SAA deconstruction and conversion experiments; A.R. designed the ionic liquids deconstruction and conversion pipeline and contributed to the writing and editing of the manuscript; V.R.P. conducted the experiments for ionic liquids deconstruction and conversion; A.E.H.-W. and R.M.H. conducted the cell wall composition analysis; M.R.J., S.J., J.-G.C., S.P.D., and G.A.T. contributed to data collection and sample processing; J.-G.C., S.P.D., and G.A.T. designed the GWAS panel, designed the approach to collect population-wide density data, and contributed to the gathering of the many samples for density measurement; B.H.D. and W.M. contributed to the conceptual design of this study on conversion and density; B.H.D. contributed to the coordination among investigators and writing and editing of the manuscript.

Notes

The authors declare no competing financial interest.

The Department of Energy will provide public access to these results of federally sponsored research in accordance with the DOE Public Access Plan (<http://energy.gov/downloads/doe-public-access-plan>).

ACKNOWLEDGMENTS

This work was supported by three U.S. Department of Energy (DOE) Bioenergy Research Centers (BRC) supported by the U.S. Department of Energy, Office of Science, Biological and

Environmental Research. It was led by the Center for Bioenergy Innovation (CBI; under FWP ERKP886), at Oak Ridge National Laboratory which is managed by UT-Battelle, LLC for the US DOE under contract number DE-AC05-00OR22725. CBI supported work at the National Laboratory of the Rockies, operated by Alliance for Sustainable Energy, LLC, for the U.S. DOE under contract no. DE-AC36-08GO28308. This material also is based upon work supported by the BRCs Great Lakes Bioenergy Research Center (GLBRC) under award number DE-SC0018409 and the Joint BioEnergy Institute (JBEI), managed by Lawrence Berkeley National Laboratory under contract AC02-05CH11231. JBEI also supported work at Sandia National Laboratories (SNL, a multimission laboratory) managed and operated by National Technology & Engineering Solutions of Sandia, LLC, a wholly owned subsidiary of Honeywell International Inc., for the U.S. DOE's National Nuclear Security Administration under contract DE-NA0003525. We thank the GLBRC Metabolomics Facility for quantification of analytes from SAA-pretreated poplar hydrolysates and the late Dr. Yaoping Zhang for his assistance with SAA pretreatment. The U.S. Government retains and the publisher, by accepting the article for publication, acknowledges that the U.S. Government retains a nonexclusive, paid-up, irrevocable, worldwide license to publish or reproduce the published form of this work, or allow others to do so, for U.S. Government purposes. The views expressed in the article do not necessarily represent the views of the DOE or the U.S. Government.

REFERENCES

- (1) *BETO: Billion-Ton 2023*; Department of Energy; <https://www.energy.gov/eere/bioenergy/2023-billion-ton-report-assessment-us-renewable-carbon-resources> (accessed 2025-08-07).
- (2) Toillon, J.; Fichot, R.; Dallé, E.; Berthelot, A.; Brignolas, F.; Marron, N. Planting Density Affects Growth and Water-Use Efficiency Depending on Site in *Populus Deltoides* × *P. Nigra*. *For. Ecol. Manage.* **2013**, *304*, 345–354.
- (3) Truax, B.; Fortier, J.; Gagnon, D.; Lambert, F. Planting Density and Site Effects on Stem Dimensions, Stand Productivity, Biomass Partitioning, Carbon Stocks and Soil Nutrient Supply in Hybrid Poplar Plantations. *Forests* **2018**, *9* (6), 293.
- (4) Medeiros, P. L.; Silva, G. G. C.; Oliveira, E. M. M.; Ribeiro, C. O.; Silva, J. M. S.; Pimenta, A. S. Efficiency of Nutrient Use for Biomass Production of a Eucalyptus Clone as a Function of Planting Density in Short-Rotation Cropping. *Aust. For.* **2020**, *83* (2), 66–74.
- (5) Younis, M.; Alnouri, S. Y.; Abu Tarboush, B. J.; Ahmad, M. N. Renewable Biofuel Production from Biomass: A Review for Biomass Pelletization, Characterization, and Thermal Conversion Techniques. *Int. J. Green Energy* **2018**, *15* (13), 837–863.
- (6) Gong, C.; Meng, X.; Thygesen, L. G.; Sheng, K.; Pu, Y.; Wang, L.; Ragauskas, A.; Zhang, X.; Thomsen, S. T. The Significance of Biomass Densification in Biological-Based Biorefineries: A Critical Review. *Renewable and Sustainable Energy Reviews* **2023**, *183*, No. 113520.
- (7) Zobel, B. J.; van Buijtenen, J. P.; Zobel, B. J.; van Buijtenen, J. P. Wood Variation and Wood Properties. *Wood variation: its causes and control*; Springer Berlin Heidelberg 1989, 132.
- (8) Zhang, S. Y.; Yu, Q.; Chauret, G.; Koubaa, A. Selection for Both Growth and Wood Properties in Hybrid Poplar Clones. *Forest Science* **2003**, *49* (6), 901–908.
- (9) Pliura, A.; Zhang, S. Y.; MacKay, J.; Bousquet, J. Genotypic Variation in Wood Density and Growth Traits of Poplar Hybrids at Four Clonal Trials. *For. Ecol. Manage.* **2007**, *238* (1–3), 92–106.

- (10) Bhat, K. M.; Bhat, K. V.; Dhamodaran, T. K. Wood Density and Fiber Length of *Eucalyptus Grandis* Grown in Kerala, India. *Wood Fiber Sci.* **1990**, *54*, 54–61.
- (11) Quilhó, T.; Miranda, I.; Pereira, H. Within-Tree Variation in Wood Fibre Biometry And Basic Density of the Urograndis Eucalypt Hybrid (*Eucalyptus Grandis* × *E. Urophylla*). *IAWA J.* **2006**, *27* (3), 243–254.
- (12) Stackpole, D. J.; Vaillancourt, R. E.; de Aguiar, M.; Potts, B. M. Age Trends in Genetic Parameters for Growth and Wood Density in *Eucalyptus Globulus*. *Tree Genet. Genomes* **2010**, *6* (2), 179–193.
- (13) Sette, C. R., Jr.; Tomazello F, M.; Lousada, J. L.; Lopes, D.; Laclau, J. P. Relationship between Climate Variables, Trunk Growth Rate and Wood Density of *Eucalyptus Grandis* W. Mill Ex Maiden Trees. *Revista Árvore* **2016**, *40* (2), 337–346.
- (14) Darmawan, W.; Rahayu, I.; Lumongga, D.; Putri, R. L.; Mubarak, M.; Gérardin, P. Selected Properties of Macassar Ebony (*Dyospiros Celebica*) from Plantation. *Journal of Tropical Forest Science* **2021**, *33* (1), 1–10.
- (15) Kiaei, M.; Kord, B.; Chehalmardian, A.; Moya, R.; Farsi, M. Mineral Content in Relation to Radial Position, Altitude, Chemical Properties and Density of Persian Ironwood. *Maderas. Ciencia y tecnología* **2015**, *17* (3), 657–672.
- (16) Magalhães, T. M. Effects of Site and Tree Size on Wood Density and Bark Properties of Lebonbo Ironwood (*Androstachys Johnsonii* Prain). *N. Z. J. For. Sci.*, **2021**, *51*, .
- (17) Gonzalez, J. S.; Kellogg, R. M.; Evaluating Wood Specific Gravity in a Tree Improvement Program. *Information report Western Forest Products Laboratory: Canada * **1978**.
- (18) Mokfienski, A.; Colodette, J. L.; Gomide, J. L.; Carvalho, A. M. M. L. Relative Importance of Wood Density and Carbohydrate Content on Pulp Yield and Product Quality. *Ciência Florestal* **2008**, *18* (3), 401.
- (19) Da, A.; Magaton, S.; Colodette, J. L.; De Fátima, A.; Gouvêa, G.; Lívio Gomide, J.; Coelho Dos, M.; Muguet, S.; Pedrazzi, C. *Eucalyptus* Wood Quality and Its Impact on Kraft Pulp Production and Use. *Tappi J.* **2009**, *32*.
- (20) Pliura, A.; Yu, Q.; Zhang, S. Y.; MacKay, J.; Périnet, P.; Bousquet, J. Variation in Wood Density and Shrinkage and Their Relationship to Growth of Selected Young Poplar Hybrid Crosses. *Forest Science* **2005**, *51* (5), 472–482.
- (21) Ohlsson, J. A.; Hallingbäck, H. R.; Jebrane, M.; Harman-Ware, A. E.; Shollenberger, T.; Decker, S. R.; Sandgren, M.; Rönnberg-Wästljung, A. C. Genetic Variation of Biomass Recalcitrance in a Natural *Salix Viminalis* (L.) Population. *Biotechnol. Biofuels* **2019**, *12* (1), 1–12.
- (22) Retief, E. C. L.; Stanger, T. K. Genetic Control of Wood Density and Bark Thickness, and Their Correlations with Diameter, in Pure and Hybrid Populations of *Eucalyptus Grandis* and *E. Urophylla* in South Africa. *Southern Forests: a Journal of Forest Science* **2009**, *71* (2), 147–153.
- (23) Grattapaglia, D.; Bertolucci, F. L.; Penchel, R.; Sederoff, R. R. Genetic Mapping of Quantitative Trait Loci Controlling Growth and Wood Quality Traits in *Eucalyptus Grandis* Using a Maternal Half-Sib Family and RAPD Markers. *Genetics* **1996**, *144* (3), 1205–1214.
- (24) Zhang, S. Y.; Morgenstern, E. K. Genetic Variation and Inheritance of Wood Density in Black Spruce (*Picea Mariana*) and Its Relationship with Growth: Implications for Tree Breeding. *Wood Sci. Technol.* **1995**, *30* (1), 63–75.
- (25) Vargas-Hernandez, J.; Adams, W. T. Genetic Variation of Wood Density Components in Young Coastal Douglas-Fir: Implications for Tree Breeding. *Can. J. For. Res.* **1991**, *21* (12), 1801–1807.
- (26) Hannrup, B.; Ekberg, I. Age-Age Correlations for Tracheid Length and Wood Density in *Pinus Sylvestris*. *Can. J. For. Res.* **1998**, *28* (9), 1373–1379.
- (27) Cornelius, J. Heritabilities and Additive Genetic Coefficients of Variation in Forest Trees. *Can. J. For. Res.* **1994**, *24* (2), 372–379.
- (28) Addison, B.; Bu, L.; Bharadwaj, V.; Crowley, M. F.; Harman-Ware, A. E.; Crowley, M. F.; Bomble, Y. J.; Ciesielski, P. N. Atomistic, Macromolecular Model of the Populus Secondary Cell Wall Informed by Solid-State NMR. *Sci. Adv.* **2024**, *10* (1), 7965.
- (29) Zhao, C.; Shao, Q.; Chundawat, S. P. S. Recent Advances on Ammonia-Based Pretreatments of Lignocellulosic Biomass. *Bioresour. Technol.* **2020**, *298*, No. 122446.
- (30) Colussi, F.; Rodríguez, H.; Michelin, M.; Teixeira, J. A. Challenges in Using Ionic Liquids for Cellulosic Ethanol Production. *Molecules* **2023**, *28* (4), 1620.
- (31) Haykir, N. I.; Nizan Shikh Zahari, S. M. S.; Harirchi, S.; Sar, T.; Awasthi, M. K.; Taherzadeh, M. J. Applications of Ionic Liquids for the Biochemical Transformation of Lignocellulosic Biomass into Biofuels and Biochemicals: A Critical Review. *Biochem. Eng. J.* **2023**, *193*, No. 108850.
- (32) Yao, A.; Choudhary, H.; Mohan, M.; Rodriguez, A.; Magurudeniya, H.; Pelton, J. G.; George, A.; Simmons, B. A.; Gladden, J. M. Can Multiple Ions in an Ionic Liquid Improve the Biomass Pretreatment Efficacy? *ACS Sustainable Chem. Eng.* **2021**, *9* (12), 4371–4376.
- (33) Barten, L. M.; Crandall, J. G.; Xie, D.; Serate, J.; Handowski, E.; Jen, A.; Overmyer, K. A.; Coon, J. J.; Hittinger, C. T.; Landick, R.; Zhang, Y.; Sato, T. K. PH Adjustment Increases Biofuel Production from Inhibitory Switchgrass Hydrolysates. *bioRxiv* **2025**, *432*, 132651.
- (34) Elgharbawy, A. A.; Alam, M. Z.; Moniruzzaman, M.; Goto, M. Ionic Liquid Pretreatment as Emerging Approaches for Enhanced Zymatic Hydrolysis of Lignocellulosic Biomass. *Biochem. Eng. J.* **2016**, *109*, 252–267.
- (35) Zhang, Y.; Oates, L. G.; Serate, J.; Xie, D.; Pohlmann, E.; Bukhman, Y. V.; Karlen, S. D.; Young, M. K.; Higbee, A.; Eilert, D.; Sanford, G. R.; Piotrowski, J. S.; Cavalier, D.; Ralph, J.; Coon, J. J.; Sato, T. K.; Ong, R. G. Diverse Lignocellulosic Feedstocks Can Achieve High Field-Scale Ethanol Yields While Providing Flexibility for the Biorefinery and Landscape-Level Environmental Benefits. *GCB Bioenergy* **2018**, *10* (11), 825–840.
- (36) Sundstrom, E.; Yaegashi, J.; Yan, J.; Masson, F.; Papa, G.; Rodriguez, A.; Mirsiaghi, M.; Liang, L.; He, Q.; Tanjore, D.; Pray, T. R.; Singh, S.; Simmons, B.; Sun, N.; Magnuson, J.; Gladden, J. Demonstrating a Separation-Free Process Coupling Ionic Liquid Pretreatment, Saccharification, and Fermentation with *Rhodospiridium Toruloides* to Produce Advanced Biofuels. *Green Chem.* **2018**, *20* (12), 2870–2879.
- (37) Evans, L. M.; Slavov, G. T.; Rodgers-Melnick, E.; Martin, J.; Ranjan, P.; Muchero, W.; Brunner, A. M.; Schackwitz, W.; Gunter, L.; Chen, J.-G.; Tuskan, G. A.; DiFazio, S. P. Population Genomics of *Populus Trichocarpa* Identifies Signatures of Selection and Adaptive Trait Associations. *Nat. Genet.* **2014**, *46* (10), 1089–1096.
- (38) Decker, S. R.; Carlile, M.; Selig, M. J.; Doeppeke, C.; Davis, M.; Sykes, R.; Turner, G.; Ziebell, A. Reducing the Effect of Variable Starch Levels in Biomass Recalcitrance Screening. *Methods Mol. Biol.* **2012**, *908*, 181–195.
- (39) Muchero, W.; Guo, J.; DiFazio, S. P.; Chen, J. G.; Ranjan, P.; Slavov, G. T.; Gunter, L. E.; Jawdy, S.; Bryan, A. C.; Sykes, R.; Ziebell, A.; Klápště, J.; Porth, I.; Skyba, O.; Unda, F.; El-Kassaby, Y. A.; Douglas, C. J.; Mansfield, S. D.; Martin, J.; Schackwitz, W.; Evans, L. M.; Czarnecki, O.; Tuskan, G. A. High-Resolution Genetic Mapping of Allelic Variants Associated with Cell Wall Chemistry in *Populus*. *BMC Genomics* **2015**, *16* (1), 24.
- (40) Happs, R. M.; Bartling, A. W.; Doeppeke, C.; Harman-Ware, A. E.; Clark, R.; Webb, E. G.; Bidy, M. J.; Chen, J. G.; Tuskan, G. A.; Davis, M. F.; Muchero, W.; Davison, B. H. Economic Impact of Yield and Composition Variation in Bioenergy Crops: *Populus Trichocarpa*. *Biofuels, Bioproducts and Biorefining* **2021**, *15* (1), 176–188.
- (41) Clark, R.; Webb, E. *Integrated Biomass Supply Analysis and Logistics Model (IBSAL) 2.0*; Oak Ridge National Laboratory **2024**. .
- (42) Chandrasekar, M.; Joshi, L.; Krieg, K.; Chipkar, S.; Burke, E.; Debrauske, D. J.; Thelen, K. D.; Sato, T. K.; Ong, R. G. A High Solids Field-to-Fuel Research Pipeline to Identify Interactions between

- Feedstocks and Biofuel Production. *Biotechnol. Biofuels* **2021**, *14* (1), 1–17.
- (43) Lee, S. B.; Tremaine, M.; Place, M.; Liu, L.; Pier, A.; Krause, D. J.; Xie, D.; Zhang, Y.; Landick, R.; Gasch, A. P.; Hittinger, C. T.; Sato, T. K. Crabtree/Warburg-like Aerobic Xylose Fermentation by Engineered *Saccharomyces Cerevisiae*. *Metab. Eng.* **2021**, *68*, 119–130.
- (44) Yang, S.; Vera, J. M.; Grass, J.; Savvakis, G.; Moskvin, O. V.; Yang, Y.; McIlwain, S. J.; Lyu, Y.; Zinonos, I.; Hebert, A. S.; Coon, J. J.; Bates, D. M.; Sato, T. K.; Brown, S. D.; Himmel, M. E.; Zhang, M.; Landick, R.; Pappas, K. M.; Zhang, Y. Complete Genome Sequence and the Expression Pattern of Plasmids of the Model Ethanologen *Zymomonas Mobilis* ZM4 and Its Xylose-Utilizing Derivatives 8b and 2032. *Biotechnol. Biofuels* **2018**, *11* (1), 1–20.
- (45) Schwalbach, M. S.; Keating, D. H.; Tremaine, M.; Marner, W. D.; Zhang, Y.; Bothfeld, W.; Higbee, A.; Grass, J. A.; Cotten, C.; Reed, J. L.; da Costa Sousa, L.; Jin, M.; Balan, V.; Ellinger, J.; Dale, B.; Kiley, P. J.; Landick, R. Complex Physiology and Compound Stress Responses during Fermentation of Alkali-Pretreated Corn Stover Hydrolysate by an *Escherichia Coli* Ethanologen. *Appl. Environ. Microbiol.* **2012**, *78* (9), 3442–3457.
- (46) Kirby, J.; Geiselman, G. M.; Yaegashi, J.; Kim, J.; Zhuang, X.; Tran-Gyamfi, M. B.; Prahl, J. P.; Sundstrom, E. R.; Gao, Y.; Munoz, N.; Burnum-Johnson, K. E.; Benites, V. T.; Baidoo, E. E. K.; Fuhrmann, A.; Seibel, K.; Webb-Robertson, B. J. M.; Zucker, J.; Nicora, C. D.; Tanjore, D.; Magnuson, J. K.; Skerker, J. M.; Gladden, J. M. Further Engineering of *R. Toruloides* for the Production of Terpenes from Lignocellulosic Biomass. *Biotechnol. Biofuels* **2021**, *14* (1), 1–16.
- (47) R Pidatala, V.; Lei, M.; Choudhary, H.; J Petzold, C.; Garcia Martin, H.; A Simmons, B.; Gladden, J.; Rodriguez, A. *Feedstocks-to-Fuels Pipeline (F2F) V1*; protocols.io 2023, .
- (48) Pidatala, V. R.; Lei, M.; Choudhary, H.; Petzold, C. J.; Garcia Martin, H.; Simmons, B. A.; Gladden, J. M.; Rodriguez, A.; Mehmood, M. A. A Miniaturized Feedstocks-to-Fuels Pipeline for Screening the Efficiency of Deconstruction and Microbial Conversion of Lignocellulosic Biomass. *PLoS One* **2024**, *19* (10), No. e0305336.
- (49) Meuwissen, T. H. E.; Hayes, B. J.; Goddard, M. E. Prediction of Total Genetic Value Using Genome-Wide Dense Marker Maps. *Genetics* **2001**, *157* (4), 1819–1829.
- (50) Lagergren, J.; Pavicic, M.; Chhetri, H. B.; York, L. M.; Hyatt, D.; Kainer, D.; Rutter, E. M.; Flores, K.; Bailey-Bale, J.; Klein, M.; Taylor, G.; Jacobson, D.; Streich, J. Few-Shot Learning Enables Population-Scale Analysis of Leaf Traits in *Populus Trichocarpa*. *Plant Phenomics* **2023**, *5*, No. 0072.
- (51) Covarrubias-Pazaran, G. Genome-Assisted Prediction of Quantitative Traits Using the R Package *Sommer*. *PLoS One* **2016**, *11* (6), No. e0156744.
- (52) de los Campos, G.; Hickey, J. M.; Pong-Wong, R.; Daetwyler, H. D.; Calus, M. P. L. Whole-Genome Regression and Prediction Methods Applied to Plant and Animal Breeding. *Genetics* **2013**, *193* (2), 327–345.
- (53) Beaudoin, M.; Hernd Ndez, R. E.; Koubaa, A.; Assistant, G.; Poliquin, J. Interclonal, Intraclonal and Within-Tree Variation in Wood Density of Poplar Hybrid Clones. *Wood Fiber Sci.* **1992**, 147–153.
- (54) Porth, I.; Klápště, J.; Skyba, O.; Lai, B. S. K.; Galdes, A.; Muchero, W.; Tuskan, G. A.; Douglas, C. J.; El-Kassaby, Y. A.; Mansfield, S. D. *Populus Trichocarpa* Cell Wall Chemistry and Ultrastructure Trait Variation, Genetic Control and Genetic Correlations. *New Phytologist* **2013**, *197* (3), 777–790.
- (55) Zobel, B. J.; Jett, J. B.; Zobel, B. J.; Jett, J. B. *The Importance of Wood Density (Specific Gravity) and Its Component Parts*; Springer Berlin Heidelberg 1995, 7897.
- (56) Molteberg, D.; Høibø, O. Development and Variation of Wood Density, Kraft Pulp Yield and Fibre Dimensions in Young Norway Spruce (*Picea Abies*). *Wood Sci. Technol.* **2006**, *40* (3), 173–189.
- (57) Pramod, S.; Rao, K. S. Anatomical Changes During Transition from Juvenile to Adult Wood in Branch and Main Trunk Xylem of Subabul (*Leucaena Leucocephala* [Lam.] de Wit). *Journal of Sustainable Forestry* **2012**, *31* (7), 661–673.
- (58) Bajwa, D. S.; Peterson, T.; Sharma, N.; Shojaeiarani, J.; Bajwa, S. G. A Review of Densified Solid Biomass for Energy Production. *Renewable and Sustainable Energy Reviews* **2018**, *96*, 296–305.
- (59) Pirraglia, A.; Gonzalez, R.; Denig, J.; Saloni, D. Technical and Economic Modeling for the Production of Torrefied Lignocellulosic Biomass for the U.S. Densified Fuel Industry. *Bioenergy Res.* **2013**, *6* (1), 263–275.
- (60) Li, Y.; Tittmann, P.; Parker, N.; Jenkins, B. Economic Impact of Combined Torrefaction and Pelletization Processes on Forestry Biomass Supply. *GCB Bioenergy* **2017**, *9* (4), 681–693.
- (61) Schipfer, F.; Kranzl, L. Techno-Economic Evaluation of Biomass-to-End-Use Chains Based on Densified Bioenergy Carriers (DBECs). *Appl. Energy* **2019**, *239*, 715–724.
- (62) Gunukula, S.; Daigneault, A.; Boateng, A. A.; Mullen, C. A.; DeSisto, W. J.; Wheeler, M. C. Influence of Upstream, Distributed Biomass-Densifying Technologies on the Economics of Biofuel Production. *Fuel* **2019**, *249*, 326–333.
- (63) Wegrzyn, J. L.; Eckert, A. J.; Choi, M.; Lee, J. M.; Stanton, B. J.; Sykes, R.; Davis, M. F.; Tsai, C.; Neale, D. B. Association Genetics of Traits Controlling Lignin and Cellulose Biosynthesis in Black Cottonwood (*Populus Trichocarpa*, Salicaceae) Secondary Xylem. *New Phytologist* **2010**, *188* (2), 515–532.
- (64) Bdeir, R.; Muchero, W.; Yordanov, Y.; Tuskan, G. A.; Busov, V.; Gailing, O. Quantitative Trait Locus Mapping of *Populus* Bark Features and Stem Diameter. *BMC Plant Biol.* **2017**, *17* (1), 1–13.
- (65) Olson, J. R.; Jourdain, C. J.; Rousseau, R. J. Selection for Cellulose Content, Specific Gravity, and Volume in Young *Populus Deltoides* Clones. *Canadian Journal of Forest Research* **1985**, *15* (2), 393–396.
- (66) Farmer, R. E.; Wilcox, J. R. Preliminary Testing of Eastern Cottonwood Clones. *Theor. Appl. Genet.* **1968**, *38* (5), 197–201.
- (67) Farmer, R. *Variation and Inheritance of Eastern Cottonwood Growth and Wood Properties under Two Soil Moisture Regimes*; Springer-Verlag Berlin Heidelberg **1970**.
- (68) Habier, D.; Fernando, R. L.; Dekkers, J. C. M. The Impact of Genetic Relationship Information on Genome-Assisted Breeding Values. *Genetics* **2007**, *177* (4), 2389–2397.
- (69) Posey, C.; Bridgwater, F.; Buxton, J. Natural Variation in Specific Gravity, Fiber Length, and Growth Rate of Eastern Cottonwood in the Southern Great Plains. 1969, .
- (70) Ilstedt, B.; Gullberg, U. Genetic Variation in a 26-Year Old Hybrid Aspen Trial in Southern Sweden. *Scand. J. For. Res.* **1993**, *8* (1–4), 185–192.
- (71) Lin, C. Y.; Geiselman, G. M.; Liu, D.; Magurudeniya, H. D.; Rodriguez, A.; Chen, Y. C.; Pidatala, V.; Unda, F.; Amer, B.; Baidoo, E. E. K.; Mansfield, S. D.; Simmons, B. A.; Singh, S.; Scheller, H. V.; Gladden, J. M.; Eudes, A. Evaluation of Engineered Low-Lignin Poplar for Conversion into Advanced Bioproducts. *Biotechnology for Biofuels and Bioproducts* **2022**, *15* (1), 1–12.
- (72) White, D. E.; Courchene, C.; McDonough, T.; Schimleck, L.; Jones, D.; Peter, G.; Purnell, R.; Goyal, G. Effects of Specific Gravity and Wood Chemical Content on the Pulp Yield of Loblolly Pine. *Tappi J.* **2009**, *8* (4), 31–36.
- (73) Gallego-Giraldo, L.; Shadle, G.; Shen, H.; Barros-Rios, J.; Fresquet Corrales, S.; Wang, H.; Dixon, R. A. Combining Enhanced Biomass Density with Reduced Lignin Level for Improved Forage Quality. *Plant Biotechnol. J.* **2016**, *14* (3), 895–904.